RSC Advances

PAPER

View Article Online
View Journal | View Issue

Cite this: *RSC Adv.*, 2018, **8**, 41432

A fluorescent sensor constructed from nitrogen-doped carbon nanodots (N-CDs) for pH detection in synovial fluid and urea determination†

Min Chen,‡[a] Wen Wu,‡[a] Yuyuan Chen,[b] Qingqing Pan,[b] Yongzhong Chen,[c] Zongfu Zheng,[c] Yanjie Zheng,[b] Liying Huang*[b] and Shaohuang Weng *[b]

Blue luminescent nitrogen-doped carbon nanodots (N-CDs) with pH-dependent properties were prepared from citric acid (CA), glutathione (GSH), and polyethylene polyamine (PEPA) using a two-step pyrolytic route. The N-CDs showed stable and strong emission bands at approximately 455 nm under 350 nm excitation. Moreover, the fluorescence of N-CDs can be gradually decreased by gradually increasing the pH value. A good linear relationship between the fluorescence intensity of N-CDs and the pH range of 3.0–9.0 was obtained. Thus, the response mechanism of N-CDs to pH was systematically investigated. N-CDs possessed $-NH_2$, –COOH, and –CONH– as active functional groups, which allowed the variable protonation/deprotonation of N-CDs to regulate the fluorescence emission intensities under changed pH values. Furthermore, upon combining urease-catalyzed hydrolysis of urea with increased pH values, a simple but effective fluorescence assay for urea was developed. The analytical performance for urea detection was the linear range of 0 to 10 mM with a detection limit of 0.072 mM. Additionally, the fluorescent sensor based on N-CDs was successfully applied for pH detection in synovial fluid and urea determination in serum.

Received 10th October 2018
Accepted 30th November 2018

DOI: 10.1039/c8ra08406h

rsc.li/rsc-advances

Introduction

The pH level plays an important role in environmental and biological systems, especially in various pathological and physiological processes.[1] The pH of different cellular compartments, bodily fluids, organs, and cells are usually tightly regulated in homeostasis. For instance, cellular level pH, which is about 7.4, can affect biomolecular structures and enzyme activity.[2,3] If pH values are changed intracellularly, abnormal cell function or growths will occur and induce serious physiological morbidities, such as cancer and stroke.[4,5] Moreover, pH can be a key indicator or have a valuable role in the behavior of enzymes,[6] disease progression,[7] some local inflammatory diseases,[8] and cell discrimination.[9] Thus, the ability to probe pH with facile strategies can be a powerful tool in biomedical and clinical applications. In particular, various effective techniques have been developed to measure pH, especially fluorescence-based strategies using pH-sensitive fluorescent nanomaterials.[3,5,10–12] Fluorescence-based strategies are outstanding tools for sensing,[10–14] especially for pH monitoring. However, some improvements are needed for pH monitoring through fluorescence: (i) extended range of pH response, (ii) simpler preparation processes, and (iii) stability. In addition, studies have reported that pH monitoring in biomedical field lacks clinical applications, such as the direct detection of pH in tissue or body fluid.

Similar to the role of hydrogen peroxide as an intermediate product of many enzymatic reactions, variable pH values can indicate some enzyme-catalyzed reactions of urease,[15] acetyl cholinesterase[16] and glucose oxidase.[17] For example, urease catalyze and decompose urea into products of NH_4^+, HCO_3^-, and OH^-,[18] which causes the increase of pH values. Therefore, methods based on pH value monitoring should be further developed to judge the activity of urease and detect the concentration of urea. Furthermore, as an end product of protein metabolism, urea has great significance in the clinical screening of kidney diseases.[19] An increase of urea concentration from the normal serum level of 2.5–7.5 mM can be a warning sign for nephritis and renal failure. Thus, the detection of urea based on pH-induced fluctuation in fluorescent signals is an appealing work.

Several fluorescent probes, such as gold nanoclusters,[6] copper nanoclusters,[20] and CdSe/ZnS quantum dots,[21] have

[a]*Department of Orthopedic Surgery, Fujian Medical University Union Hospital, Fuzhou 350001, China*

[b]*Department of Pharmaceutical Analysis, School of Pharmacy, Fujian Medical University, Fuzhou 350122, China. E-mail: shweng@fjmu.edu.cn; fjmuhly88@sina.com*

[c]*476 Hospital of PLA, Fuzhou 350002, China*

† Electronic supplementary information (ESI) available: Stability of N-CDs in salt solution, high-resolution XPS spectra of C1s and O1s, influence of pH to pure CDs, cycle times of the reversible pH-response of N-CDs, tables of the comparison in the analytical performance of pH detection and urea determination. See DOI: 10.1039/c8ra08406h

‡ Both authors contributed equally to this work.

been developed for the sensing of urea. While, the fluorescent methods of wide linear range combined with acceptable detection limit of urea using biocompatible and inexpensive probe are still needed. Compared with other reported probes, cost effective carbon nanodots (CDs) have attracted more attention due to its promising applications in biosensing,[22] bioimaging,[23] and drug delivery.[24] Recently, a series of methods, including hydrothermal methods[1] microwave methods[25] and solid-phase synthesis[26] has been developed for the fabrication of CDs to devise novel applications. Among reported works, one of the increasing interests in CDs is the development of pH-dependent fluorescent CDs, which can widen the application of CDs in biology.[16] It is noted that the suitable modification of the surface of CDs through the introduction of active groups is an effective strategy for the preparation of pH-sensitive CDs.[27] For instance, Song *et al.* developed a hydrothermal route to prepare pH-sensitive fluorescent N, S co-doped CDs with abundant –COOH and –OH on the surface.[27] Current reported methods for pH-dependent fluorescent CDs have illustrated effectiveness; however, the cost of the operating procedure, and time consumption of these recent fabricating methods remain unsatisfactory. Thus, developing a simple method to prepare pH-sensitive CDs is crucial to expand their future applications.

Inspired by the possibility of the development of the new properties of carbon dots through heteroelement doping and groups functionalization, this work proposed pH monitoring using special designed carbon dots. pH response blue fluorescence nitrogen-doped carbon nanodots (N-CDs) were prepared with a facile two-step approach. The surface of the N-CDs was abundant with functional groups, such as $-NH_2$, –COOH, and –NHCO–, which can be protonated/deprotonated in different degrees under variable pH. The zeta-potential and the decay lifetime curve of N-CDs in solutions with different pH values were measured to investigate the pH response mechanism of N-CDs. The response performance of N-CDs to variable pH was investigated and applied to detect the pH values of synovial fluids of arthritis patients through a fluorescent strategy. Moreover, coupled with the catalytic reaction of urease to urea with increased pH, we constructed a simple yet sensitive approach for monitoring urea using N-CDs as a fluorescence probe. The current sensing technique based on N-CDs has potential in diagnosing clinically complex body fluids.

Experimental section

Materials and apparatus

All reagents were of analytical grade and used as obtained. Citric acid monohydrate (CA), reduced glutathione (GSH) and polyethylene polyamine (PEPA) were purchased from Aladdin chemical industry Co., Ltd. (Shanghai, China). Urease was purchased from Sigma-Aldrich (Shanghai, China). Other common chemical reagents, like Na_2HPO_4 and NaH_2PO_4 for phosphate buffer (PB) were purchased from Sinopharm Chemical Reagent Co. Ltd (Shanghai, China).

UV-vis absorption spectra were measured on a UV-2250 spectrophotometer (Shimadzu Corporation, Japan). The Cary Eclipse Fluorescence Spectrophotometer (Agilent Technologies, USA) was used to collect the fluorescence spectra with both excitation and emission slit widths of 5 nm. All UV-vis absorption and fluorescence measurements were performed at room temperature under ambient conditions. Fourier Transform Infrared Spectroscopy (FTIR) was collected using a NICOLET iS50 Infrared Spectroscopy (Thermo Fisher Scientific, USA). Transmission electron microscopy (TEM) images were obtained on FEI Talos F200S. Zeta-potentials and dynamic light scattering (DLS) were measured on Litesizer 500 Nanometer laser particle size analyzer (Anton Paar GmbH, Austria).

Preparation of N-CDs

N-CDs were prepared according to our reported works[28,29] with some modifications. Briefly, the mixture of 2.0 g citric acid monohydrate (CA) and 0.6 g glutathione (GSH) in a round flask were heated at 140 °C for 25 min through an oil bath. A total of 10 mL polyene polyamine (PEPA) was then added to the heated mixture, accompanied by further heating from 140 °C to 200 °C, which was maintained for 1 h. Acetone was added after the reacting solution cooled down. Subsequently, a white precipitate was obtained *via* centrifugal treatment. After dialysis for 72 h using a 2 kDa cut-off membrane, the white product was freeze-dried and obtained. N-CDs were dispersed in water to create a stock solution of 5.7 mg mL^{-1} N-CDs.

For comparison, pure carbon nanodots (pure CDs) without any heteroatom doping was prepared using simple CA as source. CA (2.0 g) was heated to 180 °C and kept for 15 min. The reacting product was cooled down and dispersed with water. Afterwards, the pH of the dispersion was modulated to 7.0 with NaOH. After dialysis using a 2 kDa cut-off membrane for 8 h, the prepared pure CDs were freeze-dried.

pH detection

First, N-CDs stock solution was diluted to be 285 μg mL^{-1} with water. Then, 40 μL diluted N-CDs was added and kept in a series of PB solutions with different pH values for 3 min. Controlled the volume of the solution to be 1 mL, the fluorescence spectrum of N-CDs in different PB solutions was tested.

Detecting the pH of human synovial fluid

The obtained human synovial fluid was centrifuged at 5000 rpm for 10 min. Then, using ultrafiltration tube with 3000 kDa cut-off, the supernatant was further centrifuged at 8000 rpm for 30 min. Afterwards, the centrifuged fluid was diluted 20 times with pure water. The 20-fold diluted human synovial fluid (480 μL) was mixed with 20 μL of the N-CDs solution diluted with water by 20-fold (285 μg mL^{-1}) for 3 min at room temperature, and then the fluorescent intensity was recorded. Each sample was tested in triplicate.

Statement

All experiments were performed in compliance with relevant laws from P. R. China. All experiments were performed in accordance with the guidelines of relevant guidelines and institutional guidelines, and experiments were approved by the

ethics committee at Fujian Medical University and 476 Hospital of PLA. Informed consents were obtained from human participants of this study.

Urea assay

N-CDs stock solution was diluted 50 times with PB (pH = 6). For urea detection, 100 μL diluted N-CDs and 300 μL urease solution (6 U mL^{-1}) in PB were placed in a series of 1 mL EP tubes. Afterward, 100 μL different concentrations of urea were added to each tube. After 45 min of reaction, the fluorescence of the mixture was measured at 365 nm.

Detecting urea in human serum

Serum was centrifuged using an ultrafiltration tube with 3000 kDa cut-off at 8000 rpm for 30 min. Then, the centrifuged fluid was diluted 20 times with PB (pH = 6.0). Moreover, N-CDs stock solution was diluted 50 times with PB (pH = 6). In a 500 μL solution, the 20-fold diluted serum (100 μL) was mixed with 300 μL urease (6 U mL^{-1}) and 100 μL 20-fold diluted N-CDs solution with PB for 45 min, and the fluorescent intensity was recorded. Each sample was tested in triplicate.

Results and discussion

Characterization of the prepared N-CDs

N-CDs can be prepared from various resources with tunable optical properties, such as fluorescent properties with different emission wavelengths.[30,31] In this study, using CA, GSH, and PEPA as original sources *via* a simple melting method, N-CDs with distinct optical properties were obtained. UV/Vis and fluorescence spectra were obtained to investigate the optical properties of the prepared N-CDs, as shown in Fig. 1A. The N-CDs showed two specific absorption peaks at 240 and 355 nm, attributed to the π–π* transition.[32] A strong fluorescence emission at 450 nm with 350 nm excitation was observed for N-CDs. The dispersion of N-CDs was yellow in daylight and blue when excited under UV (Fig. 1B). Using standard quinine sulfate in 0.1 M H_2SO_4 as reference, the quantum yield (QY) of N-CDs can be measured as 9.4% excited at 350 nm. Moreover, the relationship between excitation and emission of N-CDs was further investigated, as shown in Fig. 1C. With increasing excitation wavelength, N-CDs initially increased and then decreased fluorescence intensity with almost stable luminescence wavelength at around 455 nm, indicating an excitation-independent fluorescence behaviour.[33–35] The maximum fluorescence intensity of N-CDs was obtained under excitation at 350 nm. Furthermore, the stability and anti-photobleaching of N-CDs were studied. Under long-term storage of more than 4 months at 4 °C, N-CDs maintained more than 90% of the initial fluorescence intensity. In a series of NaCl solutions, N-CDs exhibited excellent tolerance to ionic strength, even in 1.9 M NaCl (Fig. S1†). Meanwhile, under continuous irradiation at 350 nm for 4 h, the fluorescence intensity of N-CDs only decreased 9.2% (Fig. 1D), suggesting the high photostability of N-CDs for further applications. The anti-photobleaching ability of N-CDs was comparable with several reported carbon dots, like carbon dots from hydrothermal treatment of leeks[10] or threonine,[33] and N, S co-doped carbon quantum dots obtained from hydrothermal treatment of L-cysteine and $NH_3 \cdot H_2O$.[27]

The size distribution and surface states of N-CDs were further investigated in detail. TEM imaging exhibited that N-CDs were nearly spherical and well distributed with a relatively uniform diameter of 5.6 nm (right inset of Fig. 2A). HETRM imaging of N-CDs in the inset of Fig. 2A showed a well-resolved interlayer spacing of 0.20 nm, which was ascribed to the diffraction facets of graphite carbon of (100).[36] The chemical compositions and elemental analysis of N-CDs were verified using FTIR and XPS. As demonstrated in Fig. 2B, C=O stretching vibration at 1649 cm^{-1}, N–H bending vibration at 1560 cm^{-1}, and C–NH–C stretching vibration at 1124 cm^{-1} were found, indicating the doping effect of N to N-CDs in the fabrication process. Moreover, the broad absorption bands at 3430

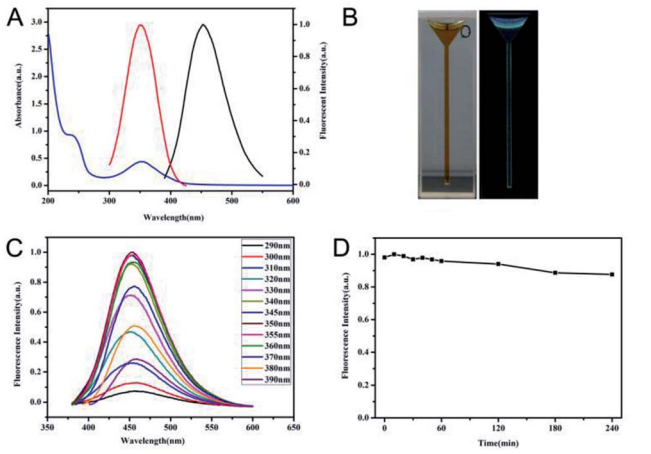

Fig. 1 Optical properties of UV/Vis and fluorescent spectra (A), appearance under visible (left) and UV (right) light (B), fluorescent spectra with different excited wavelengths (C), and the fluorescence stability with continuous irradiation at 350 nm for 4 h (D) of N-CDs.

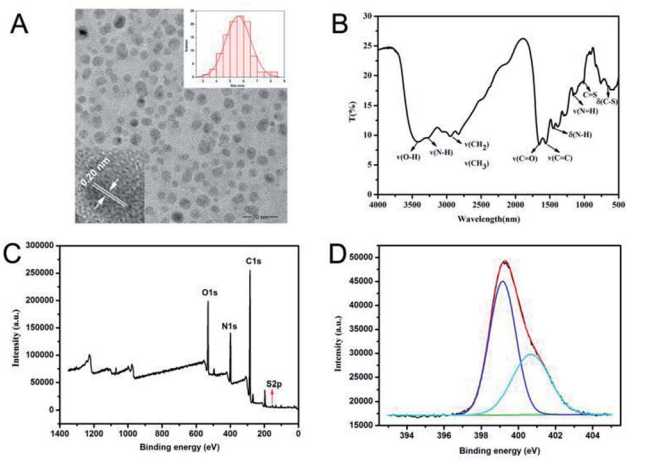

Fig. 2 TEM image (A), FTIR spectrum (B), XPS survey spectrum (C), and high-resolution XPS survey of N1s (D) of N-CDs. Insets of (A) are the HRTEM (left) and size distribution (right) of N-CDs.

and 3278 cm^{-1} ascribed to the stretching vibrations of –OH and $–NH_2$ indicated the hydrophilicity of the prepared N-CDs. Furthermore, the presence of 995 cm^{-1} corresponding to the stretching vibrations of C–S suggested the co-doping effect of S in the prepared N-CDs. The full XPS spectrum in Fig. 2C further provided and confirmed the elemental composition of N-CDs. The atomic contents of N-CDs were 67.14% carbon, 19.23% nitrogen, 13.46% oxygen, and only 0.17% sulfur. Although the reacting sources of GSH contained sulfur, the sulfur content of N-CDs was much lower than the reported fluorescent carbon nanomaterial using GSH and CA as sources.[29] The reason for the scarce sulfur content may be due to the addition of PEPA and the passivation process that occurred due to further heating at 200 °C in the fabricating process. Such a process would modify the contents of N-CDs. The high-resolution survey of C1s (Fig. S2A†) revealed the presence of C=C/C–C (graphitic or aliphatic carbon) at 284.7 eV, C–N at 285.7 eV, and C=N/C=O at 287.7 eV.[36] The N1s analysis (Fig. 2D) indicated that the forms of nitrogen in N-CDs were C–N–C (399.2 eV) and C–NH_2 (400.6 eV), thereby confirming the doping effect and formation of $–NH_2$ in N-CDs. Moreover, the O1s spectrum (Fig. S2B†) revealed two peaks of C=O at 530.9 eV and O=C–C/C=O (oxygenated carbon atoms) at 531.7 eV.[1] XPS analysis indicated that N-CDs have high percentages of nitrogen and oxygen in the forms of C=N/C–N and C=O, which were in accordance with FTIR analysis result.

Response to pH, mechanism and pH detecting performance

Considering the doping effect of nitrogen and the active surface functional groups, the response of N-CDs to various pH conditions was investigated in PB buffer with variable pH values. As shown in Fig. 3A, as pH increased from 3.0 to 12.0, a gradient decrease of fluorescence intensity of N-CDs centered at 450 nm can be observed. The fluorescence intensity remained relatively steady in the pH range of 9.0–12.0 (Fig. 3B). Meanwhile, the maximum emission wavelength of N-CDs slightly blueshifted from 485 to 445 nm when the pH values increased from 3.0 to 12.0. The blue appearance of N-CD aqueous suspension under UV irradiation was gradually enhanced whereas pH values decreased from 12.0 to 3.0, as shown in Fig. 3C. Therefore, these N-CDs could be sensitive pH indicators due to their pH-dependent fluorescence. In the pH range of 3.0–9.0, the relationship between fluorescence intensity and pH values was fitted as a linear equation of $Y = -97.924\,[\mathrm{pH}] + 1043.85$ with $R^2 = 0.9888$. The pH detection result of this method was comparable to other fluorescent pH sensors based on luminescent nanomaterials (Table S1†).

Furthermore, the mechanism of the response of N-CDs to pH was investigated. FTIR and XPS proved that N-CDs contained the active molecular functional groups of $–NH_2$, –COOH and –CONH–, which are common basic/acidic sites. These basic/acidic sites will protonate in different degrees in solutions with varying pH values. In aqueous conditions, accompanied with the increase of pH values, zeta-potentials of N-CDs gradually decreased and changed from positive to negative levels, as shown in Fig. 4A. The variable zeta-potentials of N-CDs were due to the different dissociation processes of the functional groups to modulate the protonation degree.[37] The variable protonation/deprotonation of N-CDs due to changed pH values regulated the fluorescence emission intensities. In addition, the pH response of pure CDs without doping was investigated and compared, as shown in Fig. S3.† These results showed that undoping CDs remain stable under variable pH condition. Although the undoping CDs contained –COOH on the surface, the different responses of undoping CDs and N-CDs towards pH suggested that the doping effect of nitrogen and the presence of the functional groups $–NH_2$ and –CONH– were significant factors for pH dependency. Different degrees of possible proton transfer from protonated/deprotonated nitrogen to the conjugated carbon structure under variable pH affected the energy bands of N-CDs with changes in pH, leading to different fluorescence intensities of N-CDs.[37] For further understanding of the mechanism, fluorescence decay curves of N-CDs in different pH values were investigated, as shown in Fig. 4B. The average lifetime of N-CDs was 5.28 ns in pH 3.0, 3.90 ns in pH 7.0, 3.75 ns in pH 9.0, and 3.02 ns in pH 12.0. The gradually reduced lifetime revealed that the decreased fluorescence intensities of N-CDs in higher pH condition indicated the dynamic quenching process ascribed to the increased electron-transfer process of N-CDs in increased pH conditions.[38] The above results suggested that weakened fluorescence of N-CDs in high pH conditions was due to the variable protonated/deprotonated degrees of N-

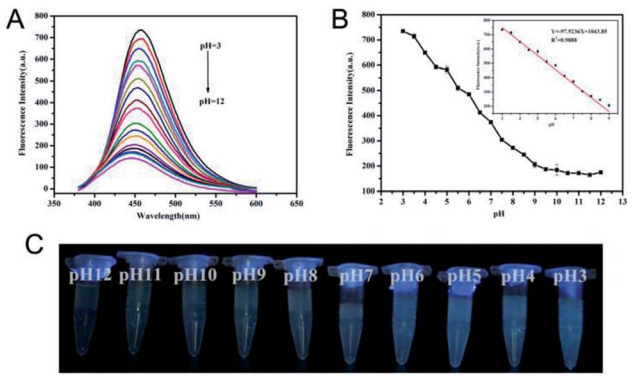

Fig. 3 Fluorescence emission spectra (A) and fluorescence images (C) of N-CDs under variable pH conditions. (B) Relationship and linear calibration equation (inset) between fluorescence intensities and pH values.

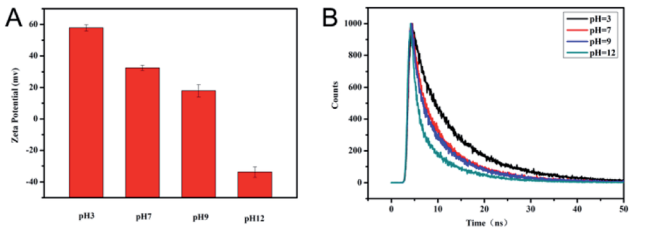

Fig. 4 Zeta-potential (A) and time-resolved fluorescence spectra (B) of N-CDs under variable pH conditions.

Table 1 Comparison of pH-sensing results in diluted synovial fluid of arthritis patients between N-CDs method and pH meter

Samples	Detected by N-CDs method	RSD (%) ($n = 3$)	Detected by pH meter	Relative errors (%)
1	7.36	2.50	7.63	−3.5
2	7.07	3.18	7.48	−4.1
3	7.32	7.26	7.52	−2.6
4	7.59	3.15	7.46	1.7
5	7.61	6.25	7.46	2.0
6	7.33	5.21	7.38	−0.7
7	7.66	5.16	7.47	2.5

CDs, leading to different degrees of proton transfer and electron transfer in the internal molecular orbital of N-CDs.[37–39]

Moreover, pH response reversibility of N-CDs was carried out by switching pH values of the N-CDs suspension back and forth between 9.0 and 5.0 using NaOH and HCl solutions, as shown in Fig. S4.† When changing the pH values from 9.0 to 5.0, N-CDs decreased in fluorescence intensity. Afterwards, fluorescence intensity was restored when the pH values changed from 9.0 to 5.0. This observation confirmed the fact that the pH-sensitive fluorescent response of N-CDs is due to the protonation/deprotonation of N-CDs.[32] The reversible response of N-CDs to switchable pH enables the N-CDs to act as pH-sensitive probes for biological applications.

The pH in living body fluid, such as blood and urine, is an important index of human health. In the synovial fluid, local pH value imbalance can promote the deposition of uric acid, which can eventually lead to gouty arthritis. During inflammation or infection of the joints, the cellular constituents, bacterial metabolites, and chemical composition of synovial fluid may cause local pH to change.[40] Thus, developing a specific assay for pH detection in synovial fluid is necessary. Herein, the pH values of several clinical joint fluid specimens were measured using N-CDs to verify the feasibility of their real clinical applications. The fluorescence intensity of N-CDs before and after the addition of diluted synovial fluid were measured, and pH value was calculated from the corresponding measured fluorescence intensities using the linear equation $Y = -97.924$ [pH] +1043.85. The results were compared with those of a standard pH meter, which were summarized in Table 1. The pH values detected using N-CDs with relatively low relative standard deviation (RSD) in different synovial fluids were close to the detected results of the pH meter. Furthermore, the absolute values of the relative errors were less than 4.5%, indicating the acceptable accuracy of the developed pH assay using N-CDs. The detection of pH values in real synovial fluids reflected that the proposed fluorescence assay was a promising strategy for pH detection in bodily fluids in laboratory medicine.

Detection of urea

It is known that the catalytic process of urea by urease results in the increase of pH. The application of N-CDs as a fluorescent probe to monitor the catalytic reaction of urease was

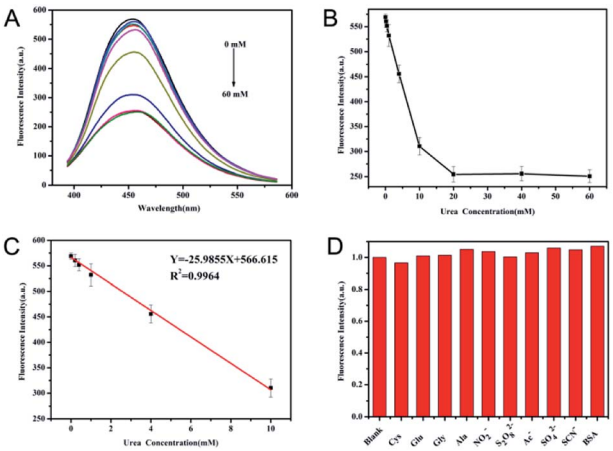

Fig. 5 Fluorescence emission spectra (A), relationship between fluorescence intensities and concentrations of urea (B) and linear calibration equation (C) of the detection of urea. (D) Normalized fluorescence response of the detection of urea and the addition of the interferents of Cys, Glu, Ala, NO_2^-, $S_2O_8^{2-}$, CH_3COO^-, SCN^-, and BSA. The detecting system contained 22.8 μg mL^{-1} N-CDs and 3.6 U mL^{-1} urease in PB in a total volume of 500 μL.

investigated. As depicted in Fig. 5A, with the increase of urea concentration from 0 to 60 mmol L^{-1} in PB containing urease and N-CDs, the fluorescence intensities of N-CDs decreased accordingly and plateaued (Fig. 5B). The observed plateau may be due to the relatively stable fluorescence intensity of N-CDs when pH values were higher than 9.0. A linear relationship between the fluorescence intensity of N-CDs and the concentration of urea in the range of 0–10 mmol L^{-1} was obtained (Fig. 5C). The fitting equation was $Y = -25.420C_{\text{urea(mmol L}^{-1})} + 566.615$ ($R^2 = 0.9983$), and the limit of detection was calculated to be 0.072 mmol L^{-1} with 3σ/slope. The analytical performance of urea determination using N-CDs in this work was comparable to recent fluorescent assay for urea (Table S2†). The limit of detection was much lower than the normal serum level of 2.5–7.5 mM in healthy human body. Furthermore, this method illustrated the characteristics of simplicity and economy.

The specificity of this method for urea was investigated using a competitive experiment. As shown in Fig. 5D, common interferents, such as glucose, cysteine, and others, have nearly no effect on the response of N-CDs towards the detection of urea, suggesting the high selectivity of this method. In addition, 2.2% RSD was obtained for the determination of 1 mmol L^{-1} urea ($n = 6$), illustrating the precision and reproducibility of this method. To evaluate the feasibility of the proposed urea fluorescence assay for practical application, the urea concentration from clinical serum samples were tested using this method. The results from this method and clinical biochemical test were summarized and compared in Table 2. The detected concentrations of the urea of serum from this assay were close to the results of clinical testing with low RSD. The absolute values of the relative errors of these two methods were less than 10%, although one result was slightly high.

Table 2 Comparison of urea detecting results in serum between N-CDs method and clinical biochemical test

Serum samples	Detected by N-CDs method (mM)	RSD (%) ($n = 3$)	Detected by biochemical analyzer (mM)	Relative errors (%)
1	12.93	0.17	13.16	−1.7
2	43.66	4.14	38.94	12.1
3	51.92	1.72	52.92	−1.9
4	11.39	2.27	10.48	8.7
5	38.05	8.84	38.94	−2.3

Conclusions

In summary, a simple and cost effective method for the fabrication N-CDs with pH-dependent properties was developed. The abundance of the active functional groups of $-NH_2$, –COOH, and –NHCO– on the surface of N-CDs allowed N-CDs to respond to varying pH values. The pH response of N-CDs was due to the variable protonation/deprotonation of N-CDs under different pH conditions. N-CDs exhibited a wide response range for pH and the possibility for accurate detection of pH values of synovial fluid of arthritis patients. Furthermore, a method for fluorescence detection based on the response of N-CDs to urea was fabricated through coupling urease catalysis to the hydrolysis of urea to modulate pH values. This method illustrated excellent performance in the detection of urea in real biological samples. This work offers a novel candidate for sensing methods constructed from the response signals from modulated pH values.

Conflicts of interest

There are no conflicts to declare.

Acknowledgements

The authors gratefully acknowledge for financial support from the National Natural Science Foundation of China (81641097, 21705021), Joint Funds for the innovation of science and Technology, Fujian province (2017Y9121, 2017Y9042), the National Science Foundation of Fujian Province (2015J01494, 2016J01767), the Elite Cultivation Program of Health and Family Planning of Fujian Province (2017-ZQN-61) and Medical Innovation Program of Fujian Province (2016-CX-44, 2018-CXB-8).

Notes and references

1 J. Shangguan, D. He, X. He, K. Wang, F. Xu, J. Liu, J. Tang, X. Yang and J. Huang, *Anal. Chem.*, 2016, **88**, 7837.
2 N. Demaurex, *News Physiol. Sci.*, 2002, **17**, 1.
3 B. Chu, H. Wang, B. Song, F. Peng, Y. Su and Y. He, *Anal. Chem.*, 2016, **88**, 9235.
4 A. Dennis, W. Rhee, D. Sotto, S. Dublin and G. Bao, *ACS Nano*, 2012, **6**, 2917.
5 Z. Wu, M. Gao, T. Wang, X. Wan, L. Zheng and C. Huang, *Nanoscale*, 2014, **6**, 3868.
6 H. Deng, G. Wu, Z. Zou, H. Peng, A. Liu, X. Lin, X. Xia and W. Chen, *Chem. Commun.*, 2015, **51**, 7847.
7 M. Yu, C. Zhou, J. Liu, J. Hankins and J. Zheng, *J. Am. Chem. Soc.*, 2011, **133**, 11014.
8 A. Lotito, M. Muscara, M. Kiss, S. Teixeira, G. Novaes, I. Laurindo, C. Silva and S. Mello, *J. Rheumatol.*, 2004, **31**, 992.
9 P. Chen, Z. Wang, S. Zong, D. Zhu, H. Chen, Y. Zhang, L. Wu and Y. Cui, *Biosens. Bioelectron.*, 2016, **75**, 446.
10 L. Shi, Y. Li, X. Li, B. Zhao, X. Wen, G. Zhang, C. Dong and S. Shuang, *Biosens. Bioelectron.*, 2016, **77**, 598.
11 K. Paek, S. Chung, C. Cho and B. Kim, *Chem. Commun.*, 2011, **47**, 10272.
12 Y. Chan, C. Wu, F. Ye, Y. Jin, P. Smith and D. Chiu, *Anal. Chem.*, 2011, **83**, 1448.
13 C. J. Kirubaharan, D. Kalpana, Y. S. Lee, A. R. Kim, D. J. Yoo, K. S. Nahm and G. G. Kumar, *Ind. Eng. Chem. Res.*, 2012, **51**, 7441.
14 S. Xavier, G. Siva, J. Annaraj, A. Kim, D. Yood and G. Gnana kumar, *Sens. Actuators, B*, 2018, **259**, 1133.
15 N. Ismail, L. Hoa, V. Huong, Y. Inoue, H. Yoshikawa, M. Saito and E. Tamiya, *Electroanalysis*, 2017, **29**, 938.
16 Y. Wang, L. Lu, H. Peng, J. Xu, F. Wang, R. Qi, A. Xu and W. Zhang, *Chem. Commun.*, 2016, **52**, 9247.
17 Y. Song, H. Liu, H. Tan, F. Xu, J. Jia, L. Zhang, Z. Li and L. Wang, *Anal. Chem.*, 2014, **86**, 1980.
18 N. Senthilkumar, G. Gnana kumar and A. Manthiram, *Adv. Energy Mater.*, 2017, **8**, 1702207.
19 K. Babu, N. Senthilkumar, A. Kim and G. Gnana kumar, *Sens. Actuators, B*, 2017, **24**, 541.
20 H. Deng, K. Li, Q. Zhuang, H. Peng, Q. Zhuang, A. Liu, X. Xia and W. Chen, *Nanoscale*, 2018, **10**, 6467.
21 C. Huang, Y. Li and T. Chen, *Biosens. Bioelectron.*, 2007, **22**, 1835.
22 X. Sun and Y. Lei, *TrAC, Trends Anal. Chem.*, 2017, **89**, 163.
23 S. Sun, L. Zhang, K. Jiang, A. Wu and H. Lin, *Chem. Mater.*, 2016, **28**, 8659.
24 S. Majumdar, G. Krishnatreya, N. Gogoi, D. Thakur and D. Chowdhury, *ACS Appl. Mater. Interfaces*, 2016, **8**, 34179.
25 S. Qu, X. Wang, Q. Lu, X. Liu and L. Wang, *Angew. Chem., Int. Ed.*, 2012, **51**, 12215.
26 H. Zhang, Y. Chen, M. Liang, L. Xu, S. Qi and H. Chen, *Anal. Chem.*, 2014, **86**, 9846.
27 Z. Song, F. Quan, Y. Xu, M. Liu, L. Cui and J. Liu, *Carbon*, 2016, **104**, 169.

28 S. Weng, D. Liang, H. Qiu, Z. Liu, Z. Lin, Z. Zheng, A. Liu, W. Chen and X. Lin, *Sens. Actuators, B*, 2015, **221**, 7.
29 Z. Liu, J. Xiao, X. Wu, L. Lin, S. Weng, M. Chen, X. Cai and X. Lin, *Sens. Actuators, B*, 2016, **229**, 217.
30 S. Zhu, Y. Song, X. Zhao, J. Shao, J. Zhang and B. Yang, *Nano Res.*, 2015, **8**, 355.
31 J. Zhou, H. Zhou, J. Tang, S. Deng, F. Yan, W. Li and M. Qu, *Microchim. Acta*, 2016, **184**, 343.
32 L. Shen, L. Zhang, M. Chen, X. Chen and J. Wang, *Carbon*, 2013, **55**, 343.
33 X. Jin, X. Sun, G. Chen, L. Ding, Y. Li, Z. Liu, Z. Wang, W. Pan, C. Hu and J. Wang, *Carbon*, 2015, **81**, 388.
34 H. Ding, S. Yu, J. Wei and H. Xiong, *ACS Nano*, 2016, **10**, 484.
35 J. Shangguan, J. Huang, D. He, X. He, K. Wang, R. Ye, X. Yang, T. Qing and J. Tang, *Anal. Chem.*, 2017, **89**, 7477.
36 H. Nie, M. Li, Q. Li, S. Liang, Y. Tan, L. Sheng, W. Shi and S. Zhang, *Chem. Mater.*, 2014, **26**, 3104.
37 A. Barati, M. Shamsipu and H. Abdollahi, *Anal. Chim. Acta*, 2016, **931**, 25.
38 W. Lu, X. Gong, M. Nan, Y. Liu, S. Shuang and C. Dong, *Anal. Chim. Acta*, 2015, **898**, 116.
39 Y. Teng, X. Jia, J. Li and E. Wang, *Anal. Chem.*, 2015, **87**, 4897.
40 K. Rajamäki, T. Nordstrom, K. Nurmi, K. Åkerman, P. Kovanen, K. Öörni and K. Eklund, *J. Biol. Chem.*, 2013, **88**, 13410.